coatings

MDPI

Article

Enhancement of Human Gingival Fibroblasts Bioactivity and Proliferation on Plasma Sprayed Yttria-Stabilised Zirconia/TiO_2 Surface Coating of Titanium Alloys: An In-Vitro Study

Afida Jemat [1,*], Masfueh Razali [2,*], Yuichi Otsuka [3] and Mariyam Jameelah Ghazali [4]

[1] Institute of Informatics and Computing in Energy, Universiti Tenaga Nasional, Jalan Ikram-Uniten, Kajang 43000, Selangor, Malaysia
[2] Department of Restorative Dentistry, Faculty of Dentistry, Universiti Kebangsaan Malaysia, Kuala Lumpur 50300, Selangor, Malaysia
[3] Department of System Safety, Nagaoka University of Technology, 1603-1 Kamitomioka Nagaoka, Niigata 940-2188, Japan; otsuka@vos.nagaokaut.ac.jp
[4] Centre for Materials Engineering & Smart Manufacturing, Faculty of Engineering & Built Environment, Universiti Kebangsaan Malaysia, Bangi 43600, Selangor, Malaysia; mariyam@ukm.edu.my
* Correspondence: afida.jemat@uniten.edu.my (A.J.); masfuah@ukm.edu.my (M.R.); Tel.: +60-3-92897745 (M.R.)

Abstract: Titanium-coated ceramic materials with varying roughness and surface topography have been developed and utilized in clinical trials within the realms of medical and dental implantology. The objective of this study was to assess how cellular attachment is affected by the surface porosity and roughness of the titanium alloy (Ti-6Al-4V) coated with titania (TiO_2)-reinforced yttria-stabilized zirconia (YZP). Additionally, the wettability of different types of TiO_2-coated YZP was also evaluated for its effect on cellular migration and attachment. The results showed excellent adhesion between fibroblast cells and the surface of the YZP/TiO_2 coating, with TiO_2 reinforcement exhibiting bioactive properties that promote rapid cell growth and reproduction. Despite its average micro surface roughness measuring 5.86 ± 0.36 µm, the YZP/TiO2 surface coating demonstrated superior suitability for both fibroblast cell adhesion and the promotion of osseointegration. The YZP coating with 30% TiO_2 demonstrated the most desirable properties, significantly enhancing biocompatibility. This study can serve as a basis for determining the biocompatibility and bioactivity of the YZP/TiO_2 coating, which holds promise as a new coating material.

Keywords: bioactivity; cell proliferation; fibroblast; surface coating; TiO_2; zirconia

check for updates

Citation: Jemat, A.; Razali, M.; Otsuka, Y.; Ghazali, M.J. Enhancement of Human Gingival Fibroblasts Bioactivity and Proliferation on Plasma Sprayed Yttria-Stabilised Zirconia/TiO_2 Surface Coating of Titanium Alloys: An In-Vitro Study. *Coatings* **2023**, *13*, 1746. https://doi.org/10.3390/coatings13101746

Academic Editor: Liqiang Wang

Received: 31 July 2023
Revised: 26 September 2023
Accepted: 1 October 2023
Published: 9 October 2023

Copyright: © 2023 by the authors. Licensee MDPI, Basel, Switzerland. This article is an open access article distributed under the terms and conditions of the Creative Commons Attribution (CC BY) license (https://creativecommons.org/licenses/by/4.0/).

1. Introduction

Semi-stable zirconia material, better known as YZP, is a material that exhibits excellent mechanical properties and has the potential to replace titanium. To date, ceramic coatings such as calcium phosphate, hydroxyapatite (HA), and TiO_2 continue to hold their status as the most widely favoured bioceramic materials for treating titanium surfaces. Nevertheless, when considering bioceramic materials, hydroxyapatite (HA) is consistently recognized as the primary option due to its exceptional biological compatibility, even though its mechanical properties may not match those of TiO_2 [1]. Lee, et al. [2] conducted a study that unveiled a substantial interaction between hydroxyapatite (HA) and zirconia (ZrO_2), accelerating the degradation of HA into tricalcium phosphate (TCP). This presented a significant challenge when combining both ceramic types. The interaction of ZrO_2 with calcium oxide (CaO) in HA resulted in the formation of calcium zirconate ($CaZrO_3$), leading to hindered amplification transformation [3]. Additionally, YZP experienced reduced mechanical properties in a humid environment due to ageing or low-temperature degradation (LTD) [4]. LTD was characterised by the slow transformation of the metastable tetragonal crystal structure to a stable monoclinic structure in the presence of water or water vapour.

Furthermore, weak bioactivity properties of the YZP coating and microcrack propagation due to LTD could lead to spontaneous implant failure. Thus, there is an insufficient body of clinical data to justify the regular utilization of zirconia implants at present [5].

Zirconia exhibits significant promise as a dental implant material, particularly when applied as a coating on titanium alloy, as it enhances both hardness [6,7] and adhesion properties. Yttria-stabilized zirconia (YZP) functions as a secondary phase within the coating, facilitating uniform particle dispersion. This characteristic enhances the bond in ceramic composite coatings, such as alumina, HA/YZP/Ti-6Al-4V, and zirconia-calcium phosphate [8], consequently leading to improved mechanical properties [9]. The coating on implants has been shown to significantly improve the surface effect [10]. Intending to obtain an optimal surface condition, the selection of the coating method is very important.

Plasma spraying techniques have been widely used to form bioactive ceramic layers with superior mechanical properties. An advantage of employing this method lies in its capability to create an effective micro-rough surface [11,12] while allowing for precise adjustment of the coating thickness within the optimal ranges of 50–130 [13,14]. Consequently, this leads to an enhancement in the bond strength within the coating-substrate system [15]. In addition, this method is also proven to increase the surface effect through the existence of pores that play an important role in reducing healing time [16] after the tooth implantation process. The existence of these surface pores in the coating further facilitates the proliferation and attachment of tissue cells on the surface of the dental implant. In addition, the high interconnection between small pores in the coating provides better nutrient circulation for tissue cells [17]. Based on the research conducted by Ding, et al. [18], it is the presence of porosities with dimensions smaller than 5 μm that plays a pivotal role in promoting cell proliferation and subsequent bone tissue growth, ultimately leading to a good bond between implant material and bone. Surface roughness of materials can influence cell adhesion and proliferation, and rough surfaces are generally considered better for cells [19]. Initial cell adhesion to material surfaces is believed to take place via mechanical contact. Therefore, suitable surface roughness is very important to produce a useful mechanical link for the initial stage.

In clinical applications such as biomaterials, assessing bioactivity through simulated body fluid is important, but the safety assessment of toxicity properties is equally important. Through cytotoxicity tests, the level of toxicity can be determined and cell adhesion and proliferation on the implant surface can also be evaluated [20,21]. Typically, cell culture methods are used for in vitro toxicity testing to simulate biological responses to biomaterials. The test can be conducted within a test tube or cell culture dish, in vitro or ex vivo with the presence of bacteria, under controlled condition/environment exposed to the substance. Commonly used cells for in vitro study include fibroblasts, osteoblasts, epithelial and endothelial cells. The concept of this toxicity test is simple—if the tested biomaterial is toxic, the cultured cells will die, and vice versa. The adhesion of tissue cells to biomaterial implants strongly influences their biocompatible properties, making quantitative or qualitative measurements important in screening new implant materials.

To evaluate the cell viability percentage of the YZP/TiO_2 coatings, a cytotoxicity test was carried out. Toxicity tests serve a dual purpose, encompassing the assessment of toxicity characteristics and the evaluation of cell adhesion and proliferation on the implant surface [21]. In line with that, the cell culture method was directly performed in this study. Human gingival fibroblast cells (hGF) (PCS-201-018™, ATCC®, Manassas, VA, USA) were selected due to their resemblance to the cells/tissue that the biomaterial is intended to be used with. Human gingival fibroblasts are also very easy to culture, grow rapidly, and remain consistent [22]. The test procedures in this study conform to the guidelines in ASTM F 813-83 Standard Practice for the Evaluation of Direct Contact Cell Culture of Materials for Medical Devices [23].

In short, a YZP/TiO_2 ceramic composite coating was produced through a plasma spray method to overcome the problem of low bioactivity properties of YZP and at the same time improve the mechanical properties. Furthermore, titanium, which has a rougher

surface, promotes the healing process in a shorter period. This study focused on the relationship between surface and cell attachment and cell proliferation behaviour on YZP/TiO_2 composite coatings. The improvement of these biological compatibility characteristics can prove that the YZP/TiO_2 ceramic coating has high potential in dental implant applications.

2. Materials and Methods

2.1. Powder Preparation

This study used two types of powders, YZP and TiO_2 (Inframat® Advanced Materials™ LLC, Manchester, CT, USA), which were sieved to achieve the optimal particle size, approximately 45–90 µm for plasma spraying. Then, the powder was mechanically mixed using the wet mixing method, which uses a rotating mill with zirconia ceramic balls and ethanol as a liquid medium to ensure a homogeneous powder mixture. After mixing, the powder mixture was finally dried in an oven at 100 °C for 6 h. For the substrate, titanium alloy was selected. The parameters used for the powder grinding process are shown in Table 1. These parameters were chosen based on the results of previous studies that can produce homogeneous powder [14] and uniform particle size [24]. The composition ratio consists of adding titania powder by 10%, 20%, and 30% (by weight) to zirconia powder.

Table 1. Powder processing parameter.

Parameter	Value
Velocity (r.p.m.)	100
Time for plasma spraying	3
Resting time in between spraying (min)	10
Amount of powder (g)	100
Powder to ethanol ratio	1:1

2.2. Plasma Spray Coating

The Ti-6Al-4V alloy substrates were subjected to grinding with silica carbide papers (1000 and 1200 grit), followed by immersion in an ethanol solution and drying in an air furnace at 60 °C for 10 min to remove surface impurities. The plates were subjected to alumina powder grit blasting (400–600 µm) to improve the mechanical bond between the coating and the substrate [25]. The process of plasma spraying was conducted as described in Jemat, et al. [26]. All coatings have been designated according to powder composition as indicated in Table 2. For this study, the coated Ti-6Al-4V alloy was cut into thin plates measuring 150 mm × 10 mm × 3 mm.

Table 2. Types of coatings for testing.

Designation	Powder Composition
YZP	100% YZP
0.1T	90% YZP + 10%TiO_2
0.2T	80%YZP + 20%TiO_2
0.3T	70% YZP + 30%TiO_2

2.3. Surface Characterisation

All coating surfaces underwent metallographic preparation according to the ASTM E 1920-03 standard [27]. The microstructure of the polished coating was observed using a scanning electron microscope (SEM) (FEI Quanta 250 FEG SEM, Quesant Instrument Corp., Agoura Hills, CA, USA). All evaluations were carried out in accordance with the ASTM E 2109 standard [28]. The phase composition of the coating was analysed using an X-ray diffractometer (XRD), (Bruker XRD, D8 Advance, Bruker AXS GmbH, Karlsruhe, Germany) analysis at room temperature (25 °C). Surface structures were assessed utilizing Diffrac.Suite EVA (Version V4.0, Bruker AXS GmbH, Karlsruhe, Germany) software. The raw data for peak structures of each specimen were identified, cross-referenced

with the data files from the International Center for Diffraction Data within the software (Diffrac.Suite EVA), and subsequently analysed. Surface roughness (R_a) measurements were acquired in micrometres using a mechanical profilometer (Formtracer SV-C3100) with an 8 mm measuring length and a speed of 2.0 mms^{-1} in contact mode. Average readings for 10 roughness scans for each YZP/TiO_2 coated were recorded. In addition to surface roughness testing, contact angle measurements were also conducted to determine the level of surface wettability on the YZP/TiO_2 coatings using the sessile drop method. The assessment of material wettability involved determining the static water contact angle on samples utilizing an optical contact angle instrument (OCA 15EC, Dataphysics Instruments GmbH, Filderstadt, Germany). The contact angles were measured using the sessile drop technique, employing 5 µL of deionized water as the liquid phase. A minimum of three droplets were dispensed onto various locations on the coated surface of the specimens, and the contact angle was gauged on each side of the droplet using SCA20 software version 2.04, Built 4 (Dataphysics Instruments GmbH, Filderstadt, Germany). The three measurements were then averaged to yield a single reading for each specimen.

2.4. In Vitro Cytotoxicity Test

The cells used in this experiment were human gingival fibroblast (hGF) cells sourced from ATCC (PCS-201-018™) because of their propensity for easy adherence and rapid proliferation. The cells at the fourth passage (Figure 1) were used in this experiment to avoid any influence from morphological changes observed in older cells. Passage 4 represents a stage where cells have matured and reached a confluent level of 80%–90% [29,30], and using cells at this stage promotes increased cell proliferation for biomaterials. The fibroblast cells were cultured in complete growth media made from Dulbecco's Modified Eagle Medium (DMEM) supplemented with 10% foetal bovine serum (FBS), 1% of 50 U/mL penicillin, 50 U/mL streptomycin, and 1% glutamine. All chemicals were from Gibco®, Thermo Fisher Scientific, Inc., Waltham, MA, USA. The cells were kept in an incubator at 37 °C and 5% CO_2.

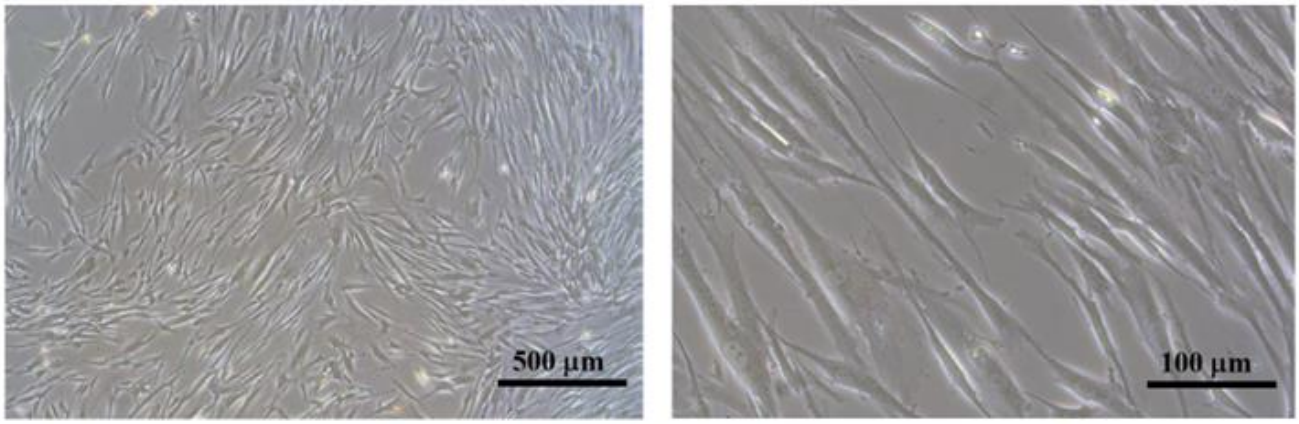


Figure 1. Fibroblast cells that have reached 80% confluence (passage 4).

To prepare for the cell culture experiment, the plate-shaped specimens (150 mm × 10 mm × 3 mm) were first sterilised by immersing them in a series of ascending ethanol solutions (70%, 80%, and 90%) mixed with distilled water and soaked for 48 h. The specimens were further subjected to ultraviolet irradiation for 30 min to prevent contamination. Then, the hGF cells were seeded on the surface of the specimens in 6-well plates. The cells were placed at a density of 5000 cells/cm^2 with 0.5 mL of the culture media. The 6-well plate was incubated for at least 3 h to allow cell attachment, and afterwards, 5 mL of culture media was added to each well. Each specimen was triplicated for each immersion period (3, 24, and 48 h) to analyse cell proliferation.

2.5. Cell Attachment and Cell Proliferation Analysis

The quantitative analysis of hGF cell adhesion on the surface of the YZP/TiO_2 coating was performed through a direct method. After 3 h of incubation, and once the cells had attached and proliferated onto the coated samples, they were removed from the culture media and washed three times using phosphate buffer saline (PBS) (Gibco®, Thermo Fisher Scientific, Inc., Waltham, MA, USA) to remove non-adherent cells. The cell viability was assessed by treating each well with 10 µL of 3-[4,5-dimethylthiazol-2-yl]-2,5-diphenyltetrazolium bromide (MTT) reagent (Biotium Inc., Hayward, CA, USA) for 4 h at 37 °C. Subsequently, 200 µL of dimethyl sulfoxide (DMSO) (Sigma-Aldrich, St. Louis, MO, USA) was added to each well to halt the MTT reaction. The absorbance was measured using a microplate reader (Tecan Infinite® 200 Pro, Tecan System, Inc., San Jose, CA, USA) set to a test wavelength of 590 nm and a reference wavelength of 630 nm. The optical density for each sample was then converted into percentage values relative to the control values in accordance with the ISO 10993-5:2009 standard [31]. The cell viability (%) was calculated using the method described by Mat-Baharin, et al. [32].

Furthermore, the human gingival fibroblasts cultured on the specimens were subjected to incubation for both 3 h and 48 h, after which they were fixed using the McDowell–Trump solution. For the assessment of biological specimens, the specimens were prepared for SEM examination employing the hexamethyldisilazane (HMDS) technique. The specimens underwent gold sputtering before being examined.

2.6. Statistical Analysis

All cell culture experiments were conducted in triplicate. Since most of the data in this study consisted of descriptive analyses, no statistical comparisons were performed. When applicable, findings are presented as the mean ± standard error of the mean (SEM). The values for surface roughness, wettability, and cell viability represent the mean values, but statistical tests were not conducted due to the small number of specimens.

3. Results

3.1. Surface Composition and Microstructure

3.1.1. Surface Topography

The surface characteristics of the specimens are illustrated in Figure 2, displaying the distinctive attributes of plasma-sprayed coatings. These features include splats, cracks, and micro-porosity, which are particularly noticeable in the YZP and 0.01T segments of the YZP/TiO_2 coating (cracks depicted by yellow arrows in Figure 2). Additionally, the presence of titanium particles can be observed as they disperse, flatten, and undergo rapid solidification, followed by cooling and solidification to create the lamellar structure in the YZP/TiO_2 composite coatings.

3.1.2. Phase Composition

Based on the XRD analysis depicted in Figure 3, the composite coating was found to consist of a mixture of tetragonal phase YZP (JCPDS No. 01-070-4427) and rutile phase TiO_2 (JCPDS No. 01-086-0148). Additionally, zirconium titanium oxide (ZrTiO4) (JCPDS No. 00-034-0415) was also identified in the XRD analysis due to the reaction between YZP and TiO_2 [33,34].

The highest intensity peak was dominated by tetragonal YZP. Theoretically, the tetragonal phase will be stable when it reaches a temperature between 1240–2370 °C. The application of high temperature during the plasma spray process and the presence of yttria (Y_2O_3) as a YZP stabilizer contribute to maintaining the tetragonal phase's stability, preventing it from transforming into other phases such as monoclinic or cubic, thus explaining the observation of the highest peak in both the YZP coating and the YZP/TiO_2 composite coating.

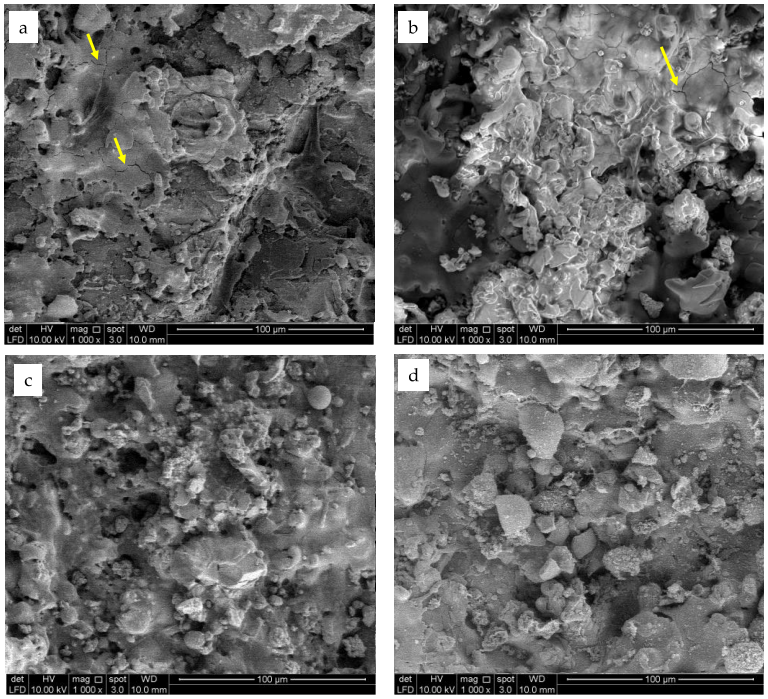


Figure 2. Surface topography of the coating for (**a**) YZP, (**b**) 0.1 T, (**c**) 0.2 T, (**d**) 0.3 T. The yellow arrows show the presence of cracks on the surface. Scale bar = 100 μm.

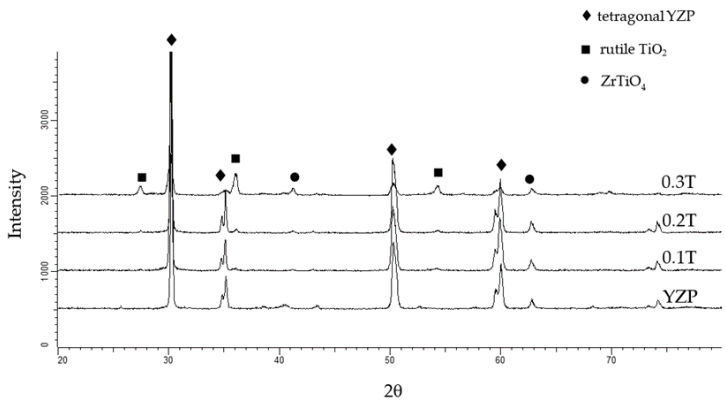


Figure 3. XRD patterns of YZP/TiO_2 composite surface coating.

3.1.3. Roughness and Wettability

As indicated in Table 3, the YZP/TiO_2 composite coating exhibits a rougher surface, with values ranging from 5.86 ± 0.36 to 9.12 ± 0.39 μm, with 0.2T being the roughest. Meanwhile, the YZP coating demonstrates the highest contact angle, indicating that it is the least hydrophilic among the four groups.

Table 3. Surface roughness and contact angle value of YZP/TiO_2 coatings.

Properties	YZP	0.01T	0.2T	0.3T
Roughness, R_a (μm)	7.06 ± 0.24	6.96 ± 0.78	9.12 ± 0.33	5.86 ± 0.29
Contact angle (°)	129.7	113.3	112.5	81.9

3.2. Cell Bioactivity

The SEM micrographs depicting cell attachment on the surface of the ceramic composite coating are shown in Figure 4. During the 3 h incubation period, hGF cells adhered

and spread efficiently on the coating's surface, appearing slender and spindle-shaped with lamellipodia, which are broader structures in some areas. From the lamellipodia, multiple protrusions, referred to as filopodia, emerged. Both lamellipodia and filopodia were labelled appropriately. In Figure 4d,g,h, blebs may also be present, indicating that cells are undergoing spreading [35] and migration (marked as red arrows). To make comparisons among the four groups, the hGF cells seeded onto 0.1T and 0.3T exhibited a richer presence of filopodia and lamellipodia and better adhesion to the substrate.

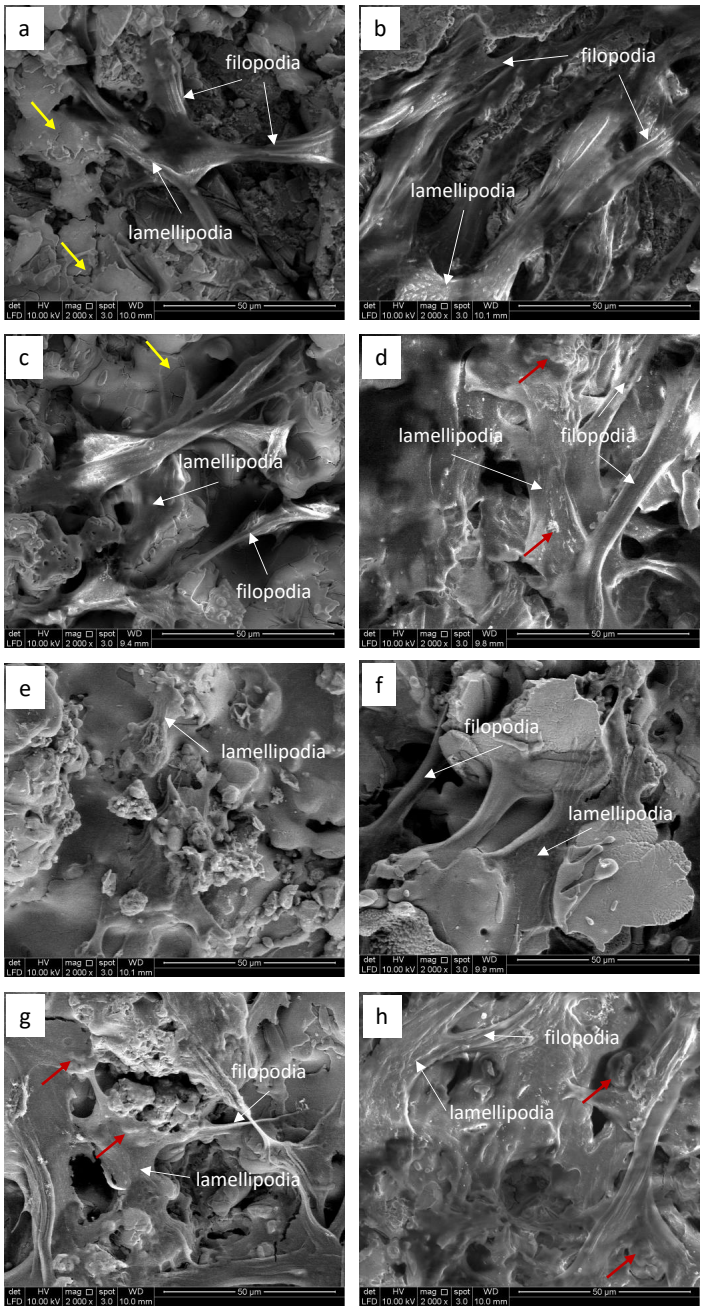


Figure 4. The SEM micrograph demonstrated the attachment of human gingival fibroblasts on the YZP coating surface at 3 h (**a**) and 48 h (**b**), respectively; on the 0.1T coating surface at 3 h (**c**) and 48 h (**d**), respectively; on the 0.2T coating surface at 3 h (**e**) and 48 h (**f**), respectively; and on the 0.3T coating surface at 3 h (**g**) and 48 h (**h**), respectively. The presence of cracks on the surface is indicated by yellow arrows, while lamellipodia and filopodia are marked with white arrows. Blebs are indicated by red arrows. Scale bar = 50 μm.

After a longer incubation period (48 h), the SEM micrographs revealed more pronounced differences. Cells seemed to occupy the surface area of the 0.3T composite coating, displaying an active filopodia structure and a flattening of the cells, which appeared well spread with long cellular extensions (Figure 4d,h). At the 48 h mark, all coatings exhibited increased cell adhesion and spreading across the entire surface, with particularly noticeable effects in the 0.1T and 0.3T composite coatings.

3.3. Cell Proliferation Analysis

Cell proliferation data for all YZP/TiO_2 composite coating compositions for 3, 24 and 48 h are presented in Figure 5. It can be observed that the rate of cell growth on the YZP single coating surface is relatively slower compared to the YZP/TiO_2 composite coating. Generally, when the incubation time increases, the percentage of cell proliferation on the coating also increases, and the cell viability on YZP and 0.2T is considered very low.

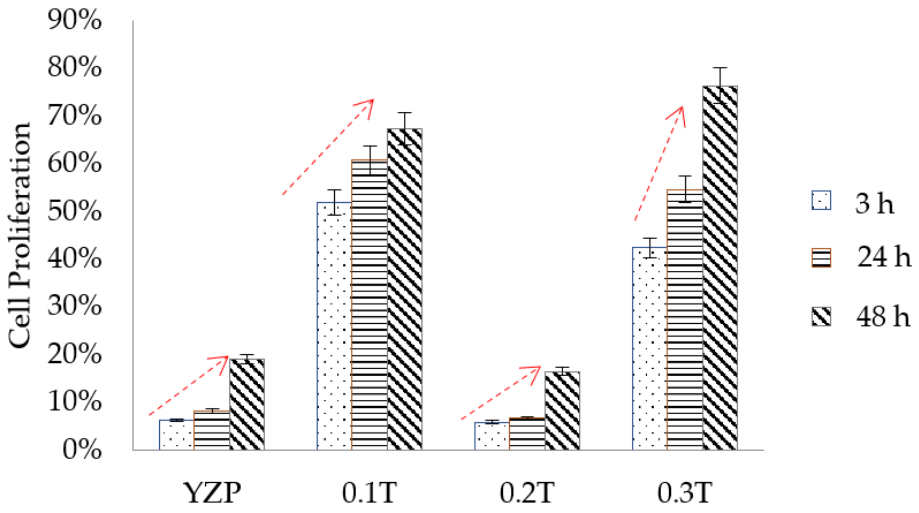


Figure 5. Cell proliferation data for YZP/TiO_2 composite coating.

4. Discussion

This study aimed to evaluate the in vitro biological response of titanium alloy (Ti-6Al-4V) coated with titania (TiO_2)-reinforced yttria-stabilized zirconia (YZP). The surface topography was measured in terms of roughness and wettability. These two aspects are the most common parameters used for the evaluation of surface properties, also closely related to each other and play an important role in influencing the bioactivity and biological compatibility of ceramic coatings [36]. The surface wettability will increase along with the reduction in the roughness value on a surface [19,37]. However, in this study, the 0.2T coating, which exhibits the highest surface roughness and displayed a slightly low wettability value with a contact angle of 112.5 ± 3.1°. According to the Cassie–Baxter model theory, surface topography has the potential to influence wettability, irrespective of the inherent wettability of the substrate material [38]. Thus, the increase in the contact angle of the 0.2T coating corresponding with its higher roughness can be explained by the water drop covering the cavities on the coating's surface, leading to reduced wettability [39]. When the contact angle value is below 90°, the surface is considered hydrophilic (exhibiting good wettability) or partially hydrophilic. Conversely, if the contact angle value exceeds 90°, the surface is categorised as hydrophobic (displaying poor wettability). In contrast, the 0.3T coating showed the best wettability properties with the lowest contact angle value of 81.9 ± 8.2°. Overall, the wettability properties of the YZP coating improved when reinforced with TiO_2. This is also supported by the findings of Noro, et al. [40] where the surface of sintered zirconia treated with alumina exhibited excellent wettability properties with a contact angle value of 80°. It is interesting to note that surface treatments or improvements to the zirconia coating are indeed able to improve the wettability properties of the material [41,42].

As shown in Table 3, the YZP/TiO_2 composite coating has a rougher surface with a value between 5.86 ± 0.36 and 9.12 ± 0.39 µm. The high value of surface roughness of YZP coating reflects the presence of unmelted powder particles [24]. Various factors such as the surface preparation process, the presence of porosity, and the distribution of cracks in the coating influence the roughness values [43]. The feature (cracks) within the coating as shown in Figure 2 may contribute to the higher surface roughness in YZP and 0.2T groups. A systematic review by Paul, et al. [44] indicated that the optimal surface roughness for the attachment and proliferation of human gingival fibroblasts falls within the range of Ra = 15 to 145 nm or Sa = 19 to 500 nm on titanium and zirconia surfaces. Correspondingly, the increase in surface roughness resulting from the plasma spraying technique employed in this study may account for the reduced viability of hGF in the YZP and 0.2T groups. The fact that the specimens underwent 30 min of ultraviolet (UV) irradiation before the cell culture experiment in this study also did not improve wettability. Theoretically, UV treatment enhances the TiO_2 surface's hydrophilicity by increasing surface free energy and removing hydrocarbons from the Ti surface, which can lead to increased migration, attachment, and proliferation of most cells [45]. However, it was reported that UV treatment of titanium alloy (Ti-6Al-4V) was able to increase surface hydrophilicity but did not influence HGF proliferation [46].

From a biological point of view, the 0.1T and 0.3T coatings showed a significant increase in cellular activities after 3 h of seeding, while the 0.2T coating exhibited relatively low cell proliferation, similar to the single YZP coating. The low proliferation value can be attributed to the relatively limited spreading of cell on the 0.2T coating (Figure 4e). Similarly, at 48 h, only the 0.1T and 0.3T composite coating surfaces showed a high level of cell proliferation. This is evident in the cell morphology observed on the surface of both coatings (Figure 4d,h), where cell growth appears robust, with cells forming a layer and covering the surface of the 0.1T and 0.3T composite coatings. In contrast to the current research, a previous study has demonstrated that human gingival fibroblast spreading and viability are enhanced on smooth zirconia surfaces with a surface roughness (R_a) of less than 0.2 µm [47].

After 48 h, the morphology on the surface of the coating displayed more filopodia, long branches, and a close adaptation to the surface, similar to the results reported by Narimatsu, et al. [48]. Micro-sized rough surfaces facilitate the attachment of active filopodia and provide strong adhesion and spreading behaviour, proving that cell growth is qualitatively better on rough surfaces. The extension of filopodia plays an important role in stabilizing fibroblast cells, allowing them to spread widely and smoothly on the surface of the implant [49,50]. However, the 0.2T coating showed slower cell growth, potentially due to its relatively high surface roughness value compared to other coatings. This may be due to the relatively high surface roughness value of 9.26 ± 0.39 µm compared to other coatings. These results are in line with previous studies that reported that surfaces with a roughness range of ~3–5 µm are excellent for fibroblast cell attachment and soft tissue growth, while rougher surfaces are more conducive to bone growth [51,52]. Besides the lowest contact angle value may be one of the factors for excellent cell adhesion on the 0.3T coating surface.

Among all coatings after 48 h, compositions of 0.1T and 0.3T exhibited the most significant development with cell proliferation increasing by 25% and 30% compared to the YZP coating. This finding is consistent with the in vitro study conducted by Bauer, et al. [53] and Zhang, et al. [54], where osteoblast cells showed excellent early adhesion and early proliferation values on TiO_2 and ZrO_2 micro surfaces compared to Ti surfaces. In summary, the incorporation of TiO_2 had a significant positive effect on cell proliferation, except for the 0.2T coating. The increase in TiO_2 with the maximum amount of 30% has shown a very bioactive surface with high wettability (81.9°), thus encouraging excellent cell adhesion compared to other surfaces. Moreover, the presence of TiO_2 increases initial cell attachment and consistently promotes cell proliferation, and this is an important factor in the successful integration of orthopaedic and dental implant osseointegration processes [55].

The morphological analysis confirmed the biocompatibility of the YZP/TiO_2 composite coating, as fibroblast cells adhered and proliferated throughout the surface, forming colonies within 24 h. The rough surface (ranging from 5.86 ± 0.36 to 7.06 ± 0.31 μm) resulting from the plasma spray process exhibits excellent cell adhesion properties and increases cell proliferation up to 30% without the need for additional surface treatment. Furthermore, the moderately roughened plasma spray surface is conducive to cell adhesion, with cell proliferation increasing by 45% in just 3 h, indicating that the surface is non-toxic and promotes strong cell adhesion. Overall, the study showed favourable cell proliferation results, confirming that the YZP/TiO_2 composite coating is non-toxic and exhibits excellent biocompatibility, although the groups with YZP coating and 0.2T show very low cell attachment and proliferation. The formation of tangled and layered cell structures on the YZP/TiO_2 composite coating indicates that this coating can promote adhesion and enhance cell proliferation.

Nevertheless, this study is not without its limitations. One of the drawbacks of the present study is that cell viability was only assessed using the monolayer cell culture technique. Future studies should also incorporate evaluations of protein and gene expressions, as well as in vivo analyses.

5. Conclusions

In this study, the plasma spray technique effectively produces a YZP ceramic composite coating reinforced with TiO_2, which has an optimal thickness ranging from approximately 50 to 130 μm, making it suitable for dental implant applications. The presence of TiO_2 in the YZP coating positively affected the bioactivity and toxicity of the material. The fibroblast cells used in the study showed biocompatibility properties to the YZP/TiO_2 coating, as cell proliferation increased with prolonged incubation time, indicating enhanced bioactivity. In conclusion, the composite coating in this study showed significantly enhanced cell attachment and cell proliferation, highlighting the excellent biocompatibility of the resulting surface.

Author Contributions: Conceptualization, A.J. and M.J.G.; methodology, A.J. and M.R.; validation, M.R., Y.O. and M.J.G.; formal analysis, A.J.; investigation, A.J.; resources, M.R. and M.J.G.; data curation, Y.O.; writing—original draft preparation, A.J.; writing—review and editing, M.R., Y.O. and M.J.G.; visualization, A.J.; supervision, M.R., Y.O. and M.J.G.; project administration, M.J.G.; funding acquisition, M.R. and M.J.G. All authors have read and agreed to the published version of the manuscript.

Funding: This research is supported by the Research University Grant of Universiti Kebangsaan Malaysia under code GUP 2019-077.

Institutional Review Board Statement: Not applicable.

Informed Consent Statement: Not applicable.

Data Availability Statement: Data presented in this study are available upon request from the corresponding author.

Acknowledgments: Special thanks are dedicated to the group of Yuichi Otsuka (Nagaoka University of Technology) for technical support by performing the plasma spray process for the coating sample.

Conflicts of Interest: The authors declare no conflict of interest. The funders had no role in the design of the study; in the collection, analyses, or interpretation of data; in the writing of the manuscript; or in the decision to publish the results.

References

1. Fathi, A.M.; Ahmed, M.K.; Afifi, M.; Menazea, A.A.; Uskoković, V. Taking hydroxyapatite-coated titanium implants two steps forward: Surface modification using graphene mesolayers and a hydroxyapatite-reinforced polymeric scaffold. *ACS Biomater. Sci. Eng.* **2021**, *7*, 360–372. [CrossRef]
2. Lee, T.M.; Yang, C.Y.; Chang, E.; Tsai, R.S. Comparison of plasma-sprayed hydroxyapatite coatings and zirconia-reinforced hydroxyapatite composite coatings: In vivo study. *J. Biomed. Mater. Res. A* **2004**, *71*, 652–660. [CrossRef] [PubMed]

3. Rapacz-Kmita, A.; Ślósarczyk, A.; Paszkiewicz, Z.; Paluszkiewicz, C. Phase stability of hydroxyapatite–zirconia (HAp–ZrO_2) composites for bone replacement. *J. Mol. Struct.* **2004**, *704*, 333–340. [CrossRef]
4. Nowicka, A.; El-Maghraby, H.F.; Švančárková, A.; Galusková, D.; Reveron, H.; Gremillard, L.; Chevalier, J.; Galusek, D. Corrosion and low temperature degradation of 3Y-TZP dental ceramics under acidic conditions. *J. Eur. Ceram. Soc.* **2020**, *40*, 6114–6122. [CrossRef]
5. Afrashtehfar, K.I.; Del Fabbro, M. Clinical performance of zirconia implants: A meta-review. *J. Prosthet. Dent.* **2020**, *123*, 419–426. [CrossRef]
6. Shahramian, K.; Gasik, M.; Kangasniemi, I.; Walboomers, X.F.; Willberg, J.; Abdulmajeed, A.; Närhi, T. Zirconia implants with improved attachment to the gingival tissue. *J. Periodontol.* **2020**, *91*, 1213–1224. [CrossRef]
7. Schünemann, F.H.; Galárraga-Vinueza, M.E.; Magini, R.; Fredel, M.; Silva, F.; Souza, J.C.M.; Zhang, Y.; Henriques, B. Zirconia surface modifications for implant dentistry. *Mater. Sci. Eng. C* **2019**, *98*, 1294–1305. [CrossRef] [PubMed]
8. Pardun, K.; Treccani, L.; Volkmann, E.; Streckbein, P.; Heiss, C.; Destri, G.L.; Marletta, G.; Rezwan, K. Mixed zirconia calcium phosphate coatings for dental implants: Tailoring coating stability and bioactivity potential. *Mater. Sci. Eng. C* **2015**, *48*, 337–346. [CrossRef]
9. Gouveia, P.F.; Mesquita-Guimarães, J.; Galárraga-Vinueza, M.E.; Souza, J.C.M.; Silva, F.S.; Fredel, M.C.; Boccaccini, A.R.; Detsch, R.; Henriques, B. In-vitro mechanical and biological evaluation of novel zirconia reinforced bioglass scaffolds for bone repair. *J. Mech. Behav. Biomed. Mater.* **2021**, *114*, 104164. [CrossRef]
10. Novaes, A.B., Jr.; de Souza, S.L.; de Barros, R.R.; Pereira, K.K.; Iezzi, G.; Piattelli, A. Influence of implant surfaces on osseointegration. *Braz. Dent. J.* **2010**, *21*, 471–481. [CrossRef] [PubMed]
11. Ghasemi, R.; Shoja-Razavi, R.; Mozafarinia, R.; Jamali, H. Laser glazing of plasma-sprayed nanostructured yttria stabilized zirconia thermal barrier coatings. *Ceram. Int.* **2013**, *39*, 9483–9490. [CrossRef]
12. Ctibor, P.; Boháč, P.; Stranyánek, M.; Čtvrtlík, R. Structure and mechanical properties of plasma sprayed coatings of titania and alumina. *J. Eur. Ceram. Soc.* **2006**, *26*, 3509–3514. [CrossRef]
13. Hung, K.-Y.; Lo, S.-C.; Shih, C.-S.; Yang, Y.-C.; Feng, H.-P.; Lin, Y.-C. Titanium surface modified by hydroxyapatite coating for dental implants. *Surf. Coat. Technol.* **2013**, *231*, 337–345. [CrossRef]
14. Khor, K.A.; Gu, Y.W.; Pan, D.; Cheang, P. Microstructure and mechanical properties of plasma sprayed HA/YSZ/Ti-6Al-4V composite coatings. *Biomaterials* **2004**, *25*, 4009–4017. [CrossRef] [PubMed]
15. Sadeghi-Fadaki, S.A.; Zangeneh-Madar, K.; Valefi, Z. The adhesion strength and indentation toughness of plasma-sprayed yttria stabilized zirconia coatings. *Surf. Coat. Technol.* **2010**, *204*, 2136–2141. [CrossRef]
16. Sennerby, L.; Dasmah, A.; Larsson, B.; Iverhed, M. Bone tissue responses to surface-modified zirconia implants: A histomorphometric and removal torque study in the rabbit. *Clin. Implant Dent. Relat. Res.* **2005**, *7*, s13–s20. [CrossRef] [PubMed]
17. Hadjicharalambous, C.; Buyakov, A.; Buyakova, S.; Kulkov, S.; Chatzinikolaidou, M. Porous alumina, zirconia and alumina/zirconia for bone repair: Fabrication, mechanical and in vitro biological response. *Biomed. Mater.* **2015**, *10*, 025012. [CrossRef]
18. Ding, S.-J.; Lee, T.-L.; Chu, Y.-H. Environmental effect on bond strength of magnetron-sputtered hydroxyapatite/titanium coatings. *J. Mater. Sci. Lett.* **2003**, *22*, 479–482. [CrossRef]
19. Romero, M.; Herrero-Climent, M.; Rios-Carrasco, B.; Brizuela, A.; Romero, M.M.; Gil, J. Investigation of the influence of roughness and dental implant design on primary stability via analysis of insertion torque and implant stability quotient: An in vitro study. *J. Clin. Med.* **2023**, *12*, 4190. [CrossRef]
20. Lugscheider, E.; Knepper, M.; Heimberg, B.; Dekker, A.; Kirkpatrick, C.J. Cytotoxicity investigations of plasma sprayed calcium phosphate coatings. *J. Mater. Sci. Mater. Med.* **1994**, *5*, 371–375. [CrossRef]
21. Shin, H.; Ko, H.; Kim, M. Cytotoxicity and biocompatibility of zirconia (Y-TZP) posts with various dental cements. *Restor. Dent. Endod.* **2016**, *41*, 167–175. [CrossRef] [PubMed]
22. Przekora, A.; Zarnowski, T.; Ginalska, G. A simple and effective protocol for fast isolation of human Tenon's fibroblasts from a single trabeculectomy biopsy—A comparison of cell behaviour in different culture media. *Cell. Mol. Biol. Lett.* **2017**, *22*, 5. [CrossRef] [PubMed]
23. *ATSM F813-83*; Standard Practice for Direct Contact Cell Culture Evaluation of Materials for Medical Devices. American Society for Testing and Materials: West Conshohocken, PA, USA, 2020.
24. Fu, L.; Khor, K.A.; Lim, J.P. Processing, microstructure and mechanical properties of yttria stabilized zirconia reinforced hydroxyapatite coatings. *Mater. Sci. Eng. A* **2001**, *316*, 46–51. [CrossRef]
25. Chou, B.-Y.; Chang, E. Microstructural characterization of plasma-sprayed hydroxyapatite–10wt% ZrO_2 composite coating on titanium. *Biomaterials* **1999**, *20*, 1823–1832. [CrossRef]
26. Jemat, A.; Ghazali, M.J.; Razali, M.; Otsuka, Y.; Rajabi, A. Effects of TiO_2 on microstructural, mechanical properties and in-vitro bioactivity of plasma sprayed yttria stabilised zirconia coatings for dental application. *Ceram. Int.* **2018**, *44*, 4271–4281. [CrossRef]
27. *ASTM E1920-03*; Standard Guide for Metallographic Preparation of Thermal Sprayed Coatings. American Society for Testing and Materials: West Conshohocken, PA, USA, 2021.
28. *ATSM E2109*; Standard Test Methods for Determining Area Percentage Porosity in Thermal Sprayed Coatings. American Society for Testing and Materials: West Conshohocken, PA, USA, 2021.

29. Keira, S.M.; Ferreira, L.M.; Gragnani, A.; Duarte, I.d.S.; Santos, I.A.N. Experimental model for fibroblast culture. *Acta Cirúrgica Bras.* **2004**, *19* (Suppl. 1), 11–16. [CrossRef]
30. Si, J.; Zhang, J.; Liu, S.; Zhang, W.; Yu, D.; Wang, X.; Guo, L.; Shen, S.G. Characterization of a micro-roughened TiO_2/ZrO_2 coating: Mechanical properties and HBMSC responses in vitro. *Acta Biochim. Biophys. Sin.* **2014**, *46*, 572–581. [CrossRef] [PubMed]
31. *ISO 10993-5*; Biological Evaluation of Medical Devices–Part 5: Tests for In Vitro Cytotoxicity. International Organization for Standardization: London, UK, 2009.
32. Mat-Baharin, N.H.; Razali, M.; Mohd-Said, S.; Syarif, J.; Muchtar, A. Influence of alloying elements on cellular response and in-vitro corrosion behavior of titanium-molybdenum-chromium alloys for implant materials. *J. Prosthodont. Res.* **2020**, *64*, 490–497. [CrossRef]
33. Miao, X.; Sun, D.; Hoo, P.W.; Liu, J.; Hu, Y.; Chen, Y. Effect of titania addition on yttria-stabilised tetragonal zirconia ceramics sintered at high temperatures. *Ceram. Int.* **2004**, *30*, 1041–1047. [CrossRef]
34. Saeidi, M.; Sarpoolaky, H.; Mirkazemi, S.M. Characterization and microstructure investigation of novel ternary ZrO_2–Al_2O_3–TiO_2 composites synthesized by citrate–nitrate process. *J. Solgel Sci. Technol.* **2015**, *76*, 436–445. [CrossRef]
35. Lee, S.Y.; Fujioka, T.; Osuga, M.; Nishimura, T.; Suetsugu, S. Lamellipodia and filopodia. In *Plasma Membrane Shaping*; Suetsugu, S., Ed.; Academic Press: Cambridge, MA, USA, 2023; pp. 245–263.
36. Stammitti-Scarpone, A.; Acosta, E.J. Solid-liquid-liquid wettability and its prediction with surface free energy models. *Adv. Colloid Interface Sci.* **2019**, *264*, 28–46. [CrossRef] [PubMed]
37. Rausch, M.A.; Shokoohi-Tabrizi, H.; Wehner, C.; Pippenger, B.E.; Wagner, R.S.; Ulm, C.; Moritz, A.; Chen, J.; Andrukhov, O. Impact of implant surface material and microscale roughness on the initial attachment and proliferation of primary human gingival fibroblasts. *Biology* **2021**, *10*, 356. [CrossRef]
38. Fan, G.; Li, F. In situ crystallization to zinc aluminate films with controlled surface microstructure and anticorrosion performance. *AIChE J.* **2012**, *58*, 2639–2649. [CrossRef]
39. Zhang, F.; Robinson, B.W.; de Villiers-Lovelock, H.; Wood, R.J.K.; Wang, S.C. Wettability of hierarchically-textured ceramic coatings produced by suspension HVOF spraying. *J. Mater. Chem. A* **2015**, *3*, 13864–13873. [CrossRef]
40. Noro, A.; Kaneko, M.; Murata, I.; Yoshinari, M. Influence of surface topography and surface physicochemistry on wettability of zirconia (tetragonal zirconia polycrystal). *J. Biomed. Mater. Res. B Appl. Biomater.* **2013**, *101*, 355–363. [CrossRef] [PubMed]
41. Yusuf, Y.; Ghazali, M.J.; Juoi, J.M.; Rahim, T.A.; Mustafa, Z. Plasma-sprayed TiO_2 coatings: Hydrophobicity enhanced by ZnO additions. *Int. J. Appl. Ceram. Technol.* **2022**, *19*, 2213–2221. [CrossRef]
42. Shanmuganantha, L.; Aslam Khan, M.U.; Sulong, A.B.; Ramli, M.I.; Baharudin, A.; Ariffin, H.M.; Abd Razak, S.I.; Ng, M.H. Characterization of titanium ceramic composite for bone implants applications. *Ceram. Int.* **2022**, *48*, 22808–22819. [CrossRef]
43. Jamhari, F.I.; Foudzi, F.M.; Buhairi, M.A.; Sulong, A.B.; Mohd Radzuan, N.A.; Muhamad, N.; Mohamed, I.F.; Jamadon, N.H.; Tan, K.S. Influence of heat treatment parameters on microstructure and mechanical performance of titanium alloy in LPBF: A brief review. *J. Mater. Res. Technol.* **2023**, *24*, 4091–4110. [CrossRef]
44. Paul, S.; Hanisch, O.; Nesic, D. Human gingival fibroblast proliferation on materials used for dental implant abutments: A systematic review. *Int. J. Prosthodont.* **2021**, *34*, 811–828. [CrossRef]
45. Razali, M.; Ngeow, W.C.; Omar, R.A.; Chai, W.L. An integrated overview of ultraviolet technology for reversing titanium dental implant degradation: Mechanism of reaction and effectivity. *Appl. Sci.* **2020**, *10*, 1654. [CrossRef]
46. Areid, N.; Peltola, A.; Kangasniemi, I.; Ballo, A.; Närhi, T.O. Effect of ultraviolet light treatment on surface hydrophilicity and human gingival fibroblast response on nanostructured titanium surfaces. *Clin. Exp. Dent. Res.* **2018**, *4*, 78–85. [CrossRef]
47. Rohr, N.; Zeller, B.; Matthisson, L.; Fischer, J. Surface structuring of zirconia to increase fibroblast viability. *Dent. Mater.* **2020**, *36*, 779–786. [CrossRef]
48. Narimatsu, I.; Atsuta, I.; Ayukawa, Y.; Oshiro, W.; Yasunami, N.; Furuhashi, A.; Koyano, K. Epithelial and connective tissue sealing around titanium implants with various typical surface finishes. *ACS Biomater. Sci. Eng.* **2019**, *5*, 4976–4984. [CrossRef] [PubMed]
49. Jacquemet, G.; Hamidi, H.; Ivaska, J. Filopodia in cell adhesion, 3D migration and cancer cell invasion. *Curr. Opin. Cell Biol.* **2015**, *36*, 23–31. [CrossRef] [PubMed]
50. Yoshihara, M.; Yamakita, Y.; Kajiyama, H.; Senga, T.; Koya, Y.; Yamashita, M.; Nawa, A.; Kikkawa, F. Filopodia play an important role in the trans-mesothelial migration of ovarian cancer cells. *Exp. Cell Res.* **2020**, *392*, 112011. [CrossRef] [PubMed]
51. Vrchovecká, K.; Kuta, J.; Uher, M.; Přibyl, J.; Pávková Goldbergová, M. Effect of titanium nanostructured surface on fibroblast behavior. *J. Biomed. Mater. Res. A* **2023**, *111*, 1333–1343. [CrossRef]
52. Van den Borre, C.E.; Zigterman, B.G.R.; Mommaerts, M.Y.; Braem, A. How surface coatings on titanium implants affect keratinized tissue: A systematic review. *J. Biomed. Mater. Res. B Appl. Biomater.* **2022**, *110*, 1713–1723. [CrossRef]
53. Bauer, S.; Park, J.; Faltenbacher, J.; Berger, S.; von der Mark, K.; Schmuki, P. Size selective behavior of mesenchymal stem cells on ZrO_2 and TiO_2 nanotube arrays. *Integr. Biol.* **2009**, *1*, 525–532. [CrossRef]

54. Zhang, S.; Sun, J.; Xu, Y.; Qian, S.; Wang, B.; Liu, F.; Liu, X. Biological behavior of osteoblast-like cells on titania and zirconia films deposited by cathodic arc deposition. *Biointerphases* **2012**, *7*, 60. [CrossRef]
55. Garcia-Gareta, E.; Hua, J.; Knowles, J.C.; Blunn, G.W. Comparison of mesenchymal stem cell proliferation and differentiation between biomimetic and electrochemical coatings on different topographic surfaces. *J. Mater. Sci. Mater. Med.* **2013**, *24*, 199–210. [CrossRef]

Disclaimer/Publisher's Note: The statements, opinions and data contained in all publications are solely those of the individual author(s) and contributor(s) and not of MDPI and/or the editor(s). MDPI and/or the editor(s) disclaim responsibility for any injury to people or property resulting from any ideas, methods, instructions or products referred to in the content.